*International Journal of Automotive Technology*, Vol. 17, No. 5, pp. 795–805 (2016)
DOI 10.1007/s12239–016–0078–x


pISSN 1229–9138/ eISSN 1976–3832

# MULTI-AXLE VEHICLE DYNAMICS STABILITY CONTROL ALGORITHM WITH ALL INDEPENDENT DRIVE WHEEL

Y. H. SHEN*, Y. GAO and T. XU

School of Mechanical Engineering, University of Science and Technology Beijing, Beijing 100083, China

*(Received 9 September 2015; Revised 25 November 2015; Accepted 16 February 2016)*

**ABSTRACT**–The stability driving characteristic and the tire wear of 8-axle vehicle with 16-independent driving wheels are discussed in this paper. The lateral stability of 8-axle vehicle can be improved by the direct yaw moment which is generated by the 16 independent driving wheels. The hierarchical controller is designed to determine the required yaw torque and driving force of each wheel. The upper level controller uses feed-forward and feed-backward control theory to obtain the required yaw torque. The fuzzification weight ratio of two control objective is built in the upper level controller to regulate the vehicle yaw and lateral motions. The rule-based yaw moment distribution strategy and the driving force adjustment based on the safety of vehicle are proposed in the lower level controller. The influence of rear steering angle is considered in the distribution of driving force of the wheel. Simulation results of a vehicle double lane change show the stability of 8-axle vehicle under the proposed control algorithm. The wear rate of tire is calculated by the interaction force between the tire and ground. The wear of tire is different from each other for the vehicle with the stability controller or not.

**KEY WORDS** : Multi-axle vehicle, Feed-forward and feedback control, Direct yaw moment control (DYC), All independent driving wheel, Wear rate of tire

## NOMENCLATURE

$m$ : vehicle mass
$k_i$ : linear cornering coefficient of the $i$ th tire
$\delta_i$ : steering angle of each axle
$l_i$ : distance between $i$ th axle and mass center
$I$ : rotational inertia of vehicle
$u$ : longitudinal velocity of vehicle
$v$ : lateral velocity
$r$ : yaw rate
$\beta$ : side-slip angle of the center of mass
$L_{i5}$ : distance between the $i$ th axle and 5th axle
$M_z$ : yaw moment
$M_{ff}$ : feed-forward yaw moment compensation
$M_{fb}$ : feed-backward yaw moment compensation
$r_d$ : ideal yaw rate
$\beta_d$ : ideal side-slip angle of center of mass
$m_i$, $n_i$ : lever arm coefficient of left and right wheel
$\delta_1$ : the inner steering angle
$B$ : wheel base
$F_{xmax}$ : maximum adhesive force of the road
$p$ : instability coefficient
$a$ : weighted coefficient
$\Delta F_b$ : the total adjustment of driving force by $p$
$\mu_s$ : coefficient of road adhesive
$F_{yi}$ : lateral force of the tire
$|\Delta\beta|$ : error of side-slip angle
$|\Delta r|$ : error of yaw rate
$F_{Zin}$ : the sum of vertical force of 8-$j$ inner wheels
$F_{Zout}$ : the sum of vertical force of 8-$j$ outer wheels
$T_{xi}$ : actual output torque of driving wheel
$F_{xi}$ : actual driving force of wheels
$F_{lim}$ : maximum driving force limited by motor
$r_r$ : rolling diameter of wheel
$W$ : frictional work of tire wear
$F_t$ : tire force acting on road
$F_x$ : longitudinal force
$F_y$ : lateral force
$V_x$ : longitudinal slip velocity of each wheel
$V_y$ : lateral slip velocity of each wheel
$\lambda$ : longitudinal slip ratio
$\alpha$ : side slip angle of the wheel
$C_0$ : tire fatigue wear
$P$ : tire vertical load
$P_0$ : tire rated load
$n$ : vertical load index
$b_x$ : relative wear coefficient by longitudinal force
$b_y$ : relative wear coefficient by lateral force
$S$ : real travelling distance
$S_0$ : standard distance
$\varepsilon$ : influence of the road
$G_{ff}$ : proportional gain coefficient of feed-forward controller
$l_{Li}$, $l_{Ri}$ : lever arm from steering wheel to vehicle mass center
$\Delta F_{Lia}$, $\Delta F_{Ria}$ : adjustment of driving force by $M_z$

*Corresponding author. e-mail: yanhua_shen@ces.ustb.edu.cn

$F_{ZLi}$, $F_{ZRi}$ : dynamic loading of the left, right wheel
$\delta_{outi}$, $\delta_{ini}$ : the outer and inner steering angle of $i$ th axle
$\Delta F_{Lib}$, $\Delta F_{Rib}$ : adjustment of driving force by $p$
$F_{Lxi}$, $F_{Rxi}$ : actual driving force of each wheel
$F_{Lxi0}$, $F_{Rxi0}$ : initial distribution driving force
$\Delta F_{Li}$, $\Delta F_{Ri}$ : adjustment of driving force

## 1. INTRODUCTION

Multi-axle vehicle is often used in the logistic, military field and other special purpose. For the shortage of fuel and strictly standard of exhaust emission, the heavy-duty vehicle manufacturers also make effort in the electrification vehicle with all independent in-wheel motor. This hybrid/ electric heavy-duty vehicle with drive controller can have many advantages such as high driving efficiency, maneuverability and stability.

The vehicle with all independent drive wheel can be accurately controlled to generate the additional yaw moment on the vehicle. This can modify the vehicle's motion, improve the handling and stability of vehicle. There are a lot of reference about improving lateral stability of the four wheel car with all independent drive wheel. Li discussed the hierarchical controller using the direct yaw moment control (DYC) to improve vehicle stability. It puts forward the feed-forward and feedback control on the required of yaw moment for 4WD car (Li *et al*., 2015). B. L. BOADA proposed a fuzzy logic controller based on the control of the vehicle yaw rate. It can allow the control of nonlinear vehicle systems with a good performance (Boada *et al*., 2005). Hasan Alipour proposed neural network observer to calculate the difference of real yaw rate and desired yaw rate (Alipour *et al*., 2014). Justin H.Sill quantified the level of lateral force saturation on each axle of a vehicle featuring an independent wheel drive system. It combines with a direct yaw-moment controller to obtain enhanced stability and responsiveness (Sill and Ayalew, 2011). Kim *et al*. (2015) compared and evaluated three different torque control algorithms for rear wheel drive electric vehicle with in-wheel motors on split-mu road. Yin (2015) presents a robust controller for four wheel independently-actuated (FWIA) electric ground vehicles to preserve vehicle stability and improve vehicle handling performance.

Some research works have been investigated in the aspect of multi-axle vehicle. The multi-axle vehicle often has double front steering axles for it possess longer rigid frame. This kind of vehicle can be easily in the instability condition when it is cornering. A generalized dynamic equation of motion was developed for the vehicle with an arbitrary number of steerable and non-steerable axles. The values for wheelbase and understeer serve to describe vehicle steady-state behavior (Williams, 2012). An *et al*. (2008) had controlled the front, middle and rear wheel steering angle and vehicle velocity. Zong *et al*. (2014) proposed a control algorithm for braking force distribution based on dynamic axle loads under non-emergency braking conditions. All these multi-axle vehicles were equipped with engine and transmission, the wheel output torque cannot be controlled independently. In order to have better performance of stability and maneuverability, Kim proposed a drive control algorithm based on optimal coordination of drive torque for an independent 8 in-wheel motor drive vehicle. The drive controller considered the variation of each wheel load conditions (Kim *et al*., 2011a, 2011b). In paper (Kim *et al*., 2011a), the distribution of each wheel driving force was determined by solving the linear matric equation. However, it only contains feedback control of the vehicle state.

And, most of references usually consider one objective, such as side-slip angle of center of mass, or the yaw rate of the vehicle. The interaction of these two objectives are not analyzed simultaneously, one variable is controlled while another variable is ignored. Although some papers discussed control two variables, the effect of large steering angle on the distribution of driver force of each wheel didn't be considered.

Moreover, the wear rate of tire for the multi-axe vehicle is another important issue. In order to decreasing the wear rate of tire, the multi-axle vehicle discussed in this paper has the rear steering axle. The multi-axle vehicle with rear steering axle may cause the vehicle bad stability and maneuverability when it driving on-road at high speed. Williams (2014) used the rear axle steer control which is a function of front axle steering input and vehicle speed to improve steady-state maneuverability and track a complex curved lane. Da Silva *et al*. (2012) has analyzed the wear rate of tire in steady-state cornering, and indicates the effects of structure parameters of the vehicle on the wear of tire. Özkan *et al*. (2014) discussed the rear steering wheels of semi-trailers to improve the maneuverability of the vehicle. It uses the minimization of tire wear as a goal to find the optimal steering mechanism for a command steer tractor semi-trailer. Zuo *et al*. (2014) uses FEA to study throughout the whole process of abnormal tire wear. Micro tread wear calculation method is described to predict the wear distribution. However, there is no related articles discusses the different driving control algorithm on the wear rate of tire. If the certain driving control algorithm causes the wear of tire much heavier than the others, it should include other objective in the evaluation of driving control algorithm.

These large heavy-duty multi-axle vehicles with all independent drive wheel should be given much attention to guarantee their driving safely and maneuverability. It is important to develop a drive controller for the 8-axle vehicle with rear steering wheel in order to improve lateral stability. This rest of paper is organized as follows. Section 2 introduces the multi-body dynamics model of 8-axle vehicle. Section 3 proposes the stability control algorithm of the vehicle, and presents the results of vehicle controlled by direct yaw moment. Section 4 compared the tire wear of

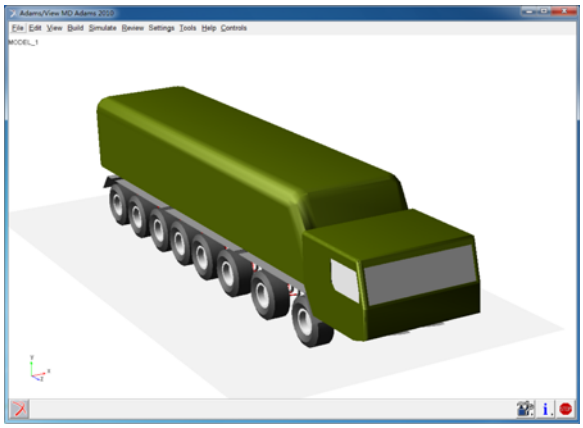

Figure 1. 8-axle vehicle dynamic model in ADAMS.

the vehicle with stability control or not. Conclusions are drawn in Section 5.

## 2. MULTI-AXLE VEHICLE DYNAMIC MODEL IN ADAMS

In order to evaluate the driving control algorithm of 8-axle all-wheel independent drive vehicle, a multi-body dynamic model is built according to the specification of the vehicle. This multi-body dynamic model is built in Adams/View which is composed of suspension, chassis, body, etc. The nonlinear characteristic of the suspension, the interactive tire-ground force are all included in the vehicle model. The vehicle possess 38 degree of freedom which includes 6 DOF of the spring mass, 16 DOF of suspension and the degree of the wheel. The tire model uses the UA model which embedded in Adams/View.

This 8-axle vehicle is driven by the 16 independent in-wheel motors which is directly connected with 2-stage hub reducer. The performance of the in-wheel motor is determined by the power requirement of the vehicle. The load transfer between the different tires will be considered in this 3-D dynamics vehicle model, and the slip dynamics characteristic of the wheel is restrained by the road friction coefficient.

## 3. MULTI-AXLE VEHICLE DRIVING CONTROL ALGORITHM BASED ON DYC

The objective of the stability control is to improve the vehicle transient response properties, enhance vehicle handling performance, and maintain stability in various maneuvers. The stability control of vehicle consists of the vehicle maneuverability and lateral stability. The maneuverability means the yaw rate tracking or small yaw rate error. The lateral stability is to have the small side-slip angle of the vehicle.

The curves in Figure 2 show the yaw rate and side-slip angle of the 8-axle vehicle at steady-state steering. As

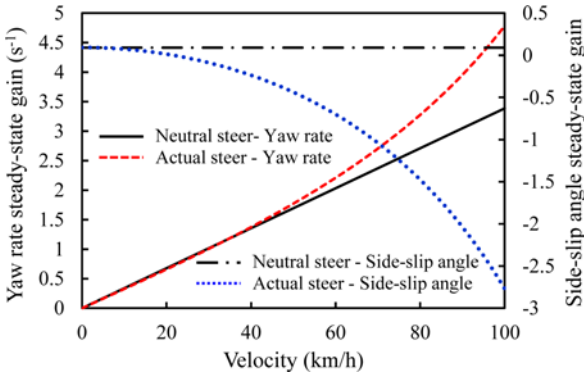


Figure 2. Steady-state gain curve of 8-axle vehicle.

shown in Figure 2, the gain ratio of actual yaw rate is higher than that of vehicle with neutral steer, so the steering characteristic of 8-axle vehicle shows the tendency of over-steer. And the gain ratio of actual side-slip angle of center of mass will increase rapidly with respect of vehicle speed. The yaw rate and side-slip angle of vehicle should be controlled simultaneously.

### 3.1. Vehicle Control Model

To compute the control yaw moment of the vehicle effectively, a reference control model for the 8-axle vehicle is built in the planar plane ignoring its pitch and roll motions.

In the 2-DOF bicycle model, the longitudinal velocity of vehicle is assumed to be constant. The longitudinal tire force is ignored and the lateral tire force of each wheel is considered as a linear dependence upon the slip angle. The vehicle model will be constructed by the forces and moments of each tire.

The dynamic variables in the 2-DOF model are the yaw rate and side-slip angle at the center of mass. The dynamic equations of the 8-axle vehicle are obtained as:

$$m(u\dot{\beta}+ur)=\sum_{i=1}^{4}k_i\left(\delta_i-\beta-\frac{l_i r}{u}\right)+\sum_{i=5}^{8}k_i\left(\delta_i-\beta+\frac{l_i r}{u}\right) \tag{1}$$

$$I\dot{r}=\sum_{i=1}^{4}l_i k_i\left(\delta_i-\beta-\frac{l_i r}{u}\right)-\sum_{i=5}^{8}l_i k_i\left(\delta_i-\beta+\frac{l_i r}{u}\right) \tag{2}$$

Apart from the non-steering wheel, the relationship of each axle steering angle with the first-axle can be expressed as;

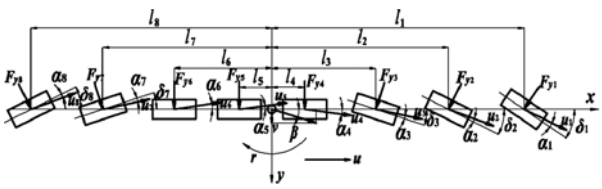

Figure 3. 2-DOF bicycle model of vehicle.

$$\delta_i = \frac{L_{i5}}{L_{15}}\delta_1 \quad (i = 2,3,7,8)$$

where, the value of $L_{15}$, $L_{25}$, $L_{35}$ are positive, the value of $L_{75}$, $L_{85}$ are negative.

Direct yaw moment (DYC) technique is used to improve high stability characteristic of the vehicle. The demanded yaw moment $M_z$ added at vehicle center of mass will be calculated by the robust controller. Equations (1) and (2) can be expressed in state space equations as follows;

$$\begin{bmatrix}\dot{\beta}\\ \dot{r}\end{bmatrix} = \begin{bmatrix}a_{11} & a_{12}\\ a_{21} & a_{22}\end{bmatrix}\begin{bmatrix}\beta\\ r\end{bmatrix} + \begin{bmatrix}b_1\\ b_2\end{bmatrix}\delta_f + \begin{bmatrix}h_1\\ h_2\end{bmatrix}M_z$$

The above equation is rewritten as;

$$\dot{X} = AX + B\delta_f + HM_z \tag{3}$$

where,

$$a_{11} = \frac{-\sum_{i=1}^{8} k_i}{mu},\quad a_{12} = \frac{-(\sum_{i=1}^{4} l_i k_i - \sum_{i=5}^{8} l_i k_i)}{mu^2} - 1$$

$$a_{21} = \frac{-(\sum_{i=1}^{4} l_i k_i - \sum_{i=5}^{8} l_i k_i)}{I_z},\quad a_{22} = \frac{-\sum_{i=1}^{8} l_i^2 k_i}{uI_z}$$

$$b_1 = \sum_{i=1}^{3}\frac{k_i L_{i5}}{muL_{15}} + \sum_{i=7}^{8}\frac{k_i L_{i5}}{muL_{15}},\quad b_2 = \sum_{i=1}^{3}\frac{l_i k_i L_{i5}}{I_z L_{15}} - \sum_{i=7}^{8}\frac{l_i k_i L_{i5}}{I_z L_{15}}$$

$$h_1 = 0,\ h_2 = 1/I_z,\ X = [\beta\ \ r]^T,\ \delta_f = \delta_1$$

The transfer function of side-slip angle of center mass and yaw rate is;

$$\beta(s) = \frac{(b_1 s - b_1 a_{22} + b_2 a_{12})\delta_f(s) + h_2 a_{12} M_z(s)}{(s - a_{11})(s - a_{22}) - a_{21}a_{12}} \tag{4}$$

$$r(s) = \frac{(b_2 s + b_1 a_{21} - b_2 a_{11})\delta_f(s) + h_2 (s - a_{11}) M_z(s)}{(s - a_{11})(s - a_{22}) - a_{21}a_{12}} \tag{5}$$

It is easy to distribute the yaw moment for the vehicle driven by independent in-wheel motor. The stability driving controller of 8-axle vehicle will be composed of hierarchy controller to ensure the vehicle following the reference yaw rate and reducing the side-slip angle. The upper level controller is designed to determine the control yaw moment $M_z$ acting on the vehicle, and the lower level controller is designed to distribute the driving force of each wheel.

### 3.2. Upper Level Controller

In the upper-level controller shown in Figure 4, feed-forward and feed-backward control theory is used to compute the required yaw moment. Yaw moment compensation $M_{ff}$ is determined by feed-forward controller, $M_{fb}$ is feed-backward control torque, $\beta_d$, $r_d$ are ideal yaw rate and side-slip angle of center of mass.

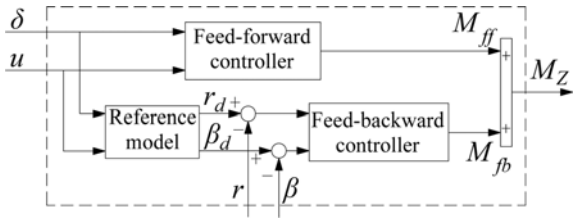


Figure 4. Schematic of upper controller.

#### 3.2.1. Feed-forward controller

The aim of feed-forward controller is to make the side-slip angle of center of mass and yaw rate tending to the ideal value. The relationship of compensation yaw moment and steering angle of the first-axle is obtained as;

$$M_{ff}(s) = G_{ff}\delta_f(s) \tag{6}$$

where, $G_{ff}$ is the proportional gain coefficient of feed-forward controller.

In the steady-state steering, if set $M_Z(s)=M_{ff}(s)$, combining Equations (4) and (6), the response of side-slip angle to the first-axle steering angle will be;

$$\frac{\beta}{\delta_f} = \frac{-b_1 a_{22} + b_2 a_{12} + h_2 a_{12} G_{ff}}{a_{11}a_{22} - a_{21}a_{12}} \tag{7}$$

The ideal side-slip angle of center mass can be simplified as;

$$\beta = \frac{l_5}{L_{15}}\delta_f \tag{8}$$

Rearranging Equations (7) and (8), the gain coefficient $G_{ff1}$ of feed-forward controller is expressed as;

$$G_{ff1} = \frac{l_5(a_{11}a_{22} - a_{21}a_{12})}{L_{15}h_2 a_{12}} + \frac{b_1 a_{22} - b_2 a_{12}}{h_2 a_{12}} \tag{9}$$

If the vehicle is controlled by the small yaw rate error, combining the Equations (5) and (6), the response of yaw rate to the first-axle steering angle will be;

$$\frac{r}{\delta_f} = \frac{b_1 a_{21} - b_2 a_{11} - h_2 a_{11} G_{ff}}{a_{11}a_{22} - a_{21}a_{12}} \tag{10}$$

And the ideal yaw rate is written as;

$$r = \frac{u}{L_{15}}\delta_f \tag{11}$$

The gain coefficient $G_{ff2}$ of feed-forward controller can be derived from the Equations (10) and (11);

$$G_{ff2} = \frac{b_1 a_{21} - b_2 a_{11}}{h_2 a_{11}} - \frac{u(a_{11}a_{22} - a_{21}a_{12})}{L_{15}h_2 a_{11}} \tag{12}$$

The required yaw moment $M_z$ will be different if the vehicle is controlled with the objectives of the side-slip angle of the center of mass and yaw rate respectively. Controlling one of these two parameters individually will

inevitably lead to variation of other parameter. The proportional gain coefficient $G_{ff}$ of feed-forward controller in Equation (6) should be determined by the combination of these two objectives.

$$G_{ff} = a \cdot G_{ff1} + (1-a) \cdot G_{ff2} \tag{13}$$

In Equation (13), $G_{ff1}$ is the gain coefficient of feed-forward controller in which the vehicle is controlled according to side-slip angle of center of mass, $G_{ff2}$ is the gain coefficient of feed-forward controller in which the vehicle is controlled according to yaw rate, $a$ is the weighted coefficient.

Figure 5 illustrates the gain coefficients $G_{ff1}$ and $G_{ff2}$ with respect of vehicle speed. As the vehicle speed lower than 33 km/h, the action directions of yaw moment on the vehicle center of mass will be opposite each other if the vehicle is controlled by the gain coefficient $G_{ff1}$ and $G_{ff2}$ respectively. In order to guarantee the 8-axle vehicle following the path accurately, it should be to mainly adjust the gain coefficient $G_{ff2}$ to make the vehicle moving in neutral steer.

On the contrary, when the vehicle speed larger than 33 km/h, the action direction of yaw moment on the vehicle will be the same for the gain coefficient $G_{ff1}$ and $G_{ff2}$. If the vehicle only adjusted by the yaw moment determined by the gain $G_{ff2}$, the characteristic of the vehicle steady-state lateral maneuver will show the neutral steer. However, the 8-axle vehicle should be under-steer at high speed in order to avoid the high sensitive about the steering wheel and guarantee the vehicle safety. In this case, it should increase the weighted coefficient of $G_{ff1}$.

Therefore, the feed-forward controller should be designed to control the yaw rate and obtain good response of the side-slip angle. The main advantage of fuzzy models is the possibility of elaborating them on the basis of fewer information about a system. The weighted coefficient $a$ in Equation (13) can be obtained by a fuzzy logic rule: the input variables of fuzzy controller are the relationship $r(1,2)$ of $G_{ff1}$, $G_{ff2}$ (opposite sign (OS), exist zero (EZ), same sign (SS)), and vehicle speed (low speed (LS), medium speed (MS), high speed (HS)); weighted

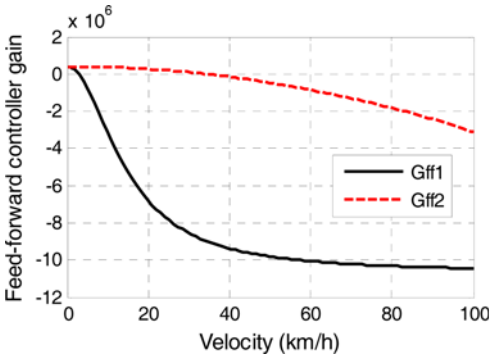


Figure 5. Feed-forward controller gain coefficients $G_{ff1}$, $G_{ff2}$.

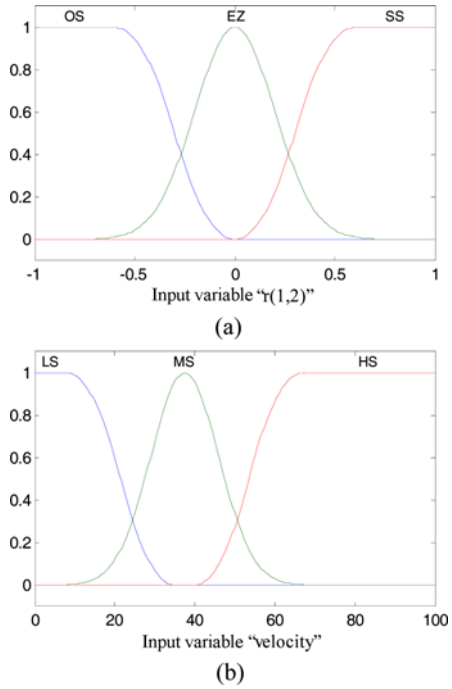


Figure 6. Fuzzy membership of input variables: $r(1,2)$, velocity of vehicle.

parameter $a$ (small (SM), relative small (RS), medium (MD), relative big (RB), big (BG)) is the output variable. The fuzzy logic adjusts $a$ depending on the $r(1,2)$ and vehicle speed.

The fuzzy sets of input and output variables are expressed as following;

$$r(1,2) = \{OS, EZ, SS\},\ u = \{LS, MS, HS\}$$

$$a = \{ZR, SM, RS, MD, RB, BG\}$$

Figure 6 shows the membership functions of two input variables as they correspond to three sets, and the membership function of outputs as they correspond to five sets. The base of the fuzzy rules is applied in Table 1.

As shown in Figure 5, the gain curve of side-slip angle is approximately quadratic function of vehicle speed while the gain curve of yaw rate is like linear function, thus the fuzzification of weighted coefficient $a$ will be like the map in Figure 7.

### 3.2.2. Reference ideal control model

Table 1. Fuzzy logic rule-based.

| $u$ \ $r(1,2)$ | OS | EZ | SS |
|---|---|---|---|
| LS | SM | RS | - |
| MS | RS | MD | RB |
| HS | - | RB | BG |

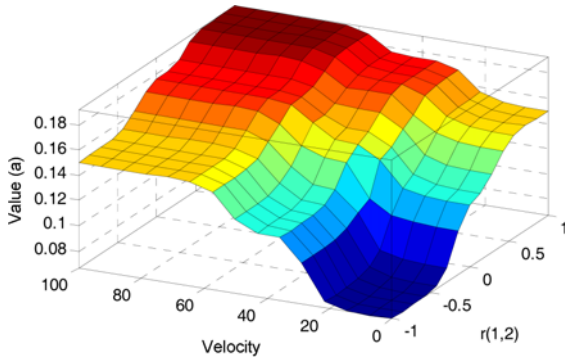


Figure 7. Fuzzification of weighted coefficient *a*.

The 2DOF vehicle model with the feedforward controller is regarded as vehicle reference ideal control model, and the ideal transfer functions of the transfer function of side-slip angle of center mass and yaw rate are as following;

$$\frac{r_d(s)}{\delta_f(s)} = \frac{(b_2 + h_2 G_{ff})s + (b_1 a_{21} - b_2 a_{11} - h_2 a_{11} G_{ff})}{s^2 - (a_{11} + a_{22})s + (a_{11} a_{22} - a_{21} a_{12})} \tag{14}$$

$$\frac{\beta_d(s)}{\delta_f(s)} = \frac{b_1 s + (b_2 a_{12} + h_2 a_{12} G_{ff} - b_1 a_{22})}{s^2 - (a_{11} + a_{22})s + (a_{11} a_{22} - a_{21} a_{12})} \tag{15}$$

Rearranging Equations (14) and (15) in a matrix form, the state equation of vehicle reference ideal control model can be expressed as;

$$\dot{X}_d = A_d X_d + B_d \delta_f \tag{16}$$

where, the desired vehicle state vector $X_d = \begin{bmatrix} \beta_d \\ r_d \end{bmatrix}$, and $A_d = \begin{bmatrix} a_{11} & a_{12} \\ a_{21} & a_{22} \end{bmatrix}$, $B_d = \begin{bmatrix} b_1 \\ b_2 + h_2 G_{ff} \end{bmatrix}$

The steady-state gains of yaw rate and side-slip angle are shown in Figure 8 after the ideal 2-DOF vehicle model (Equation (3)) controlled by the feed-forward controller. The over-steering characteristic of the vehicle will be turned into under-steer from the aspect of steady yaw rate. The gain ratio of side-slip angle will be reduced to − 1.5 from the initial value − 2.7.

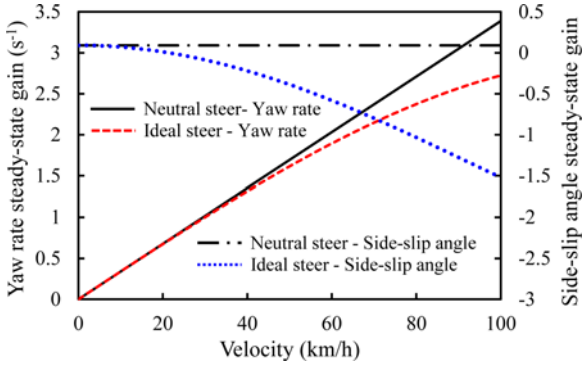


Figure 8. Steady-state gain of ideal 2DOF vehicle model after feed-forward controller.

3.2.3. Feed-backward controller

The optimal yaw moment is determined by feed-backward controller based on LQR algorithm. This optimal yaw moment is used to make the transient response of vehicle following the ideal reference model, and can resist the external disturbance.

The derivate of offset of actual and ideal state vector is given as;

$$\dot{E} = \dot{X} - \dot{X}_d \tag{17}$$

Combining the Equations (3), (16) and (17), Equation (17) will be transformed as follows;

$$\dot{E} = AE + HM_z + (B - B_d)\delta_f \tag{18}$$

The third item in Equation (18) will be interference item which caused by the 1th-axle steering angle. Let it be zero, the offset derivate Equation (17) can be rewritten as;

$$\dot{E} = AE + HM_{fb} \tag{19}$$

The yaw moment $M_{fb}$ calculated by feed-backward controller can be;

$$M_{fb} = -G_{fb}E = -[g_{fb1} \quad g_{fb2}]E \tag{20}$$

where, $g_{fb1}$ and $g_{fb2}$ are the feedback gain of actual vehicle model and ideal reference model.

Suppose minimum the performance index of vehicle, the cost function of LQR is defined as;

$$J = \int_0^\infty (e^T Q e + M_{fb1}{}^T R M_{fb1}) dt \tag{21}$$

where, $Q$ is positive and is often set as a diagonal matrix, $R$ is the penalty coefficient of control input $M_{fb}$.

The yaw moment $M_{fb}$ can be achieved by the LQR optimal control theory. Thus, the total additional yaw moment $M_z$ will be;

$$M_z = M_{ff} + M_{fb} \tag{22}$$

The feedback and feed-forward parts in the $M_z$ can adaptively control the vehicle adjusting its track for a nonlinear uncertain systems.

3.3. Lower Level Controller

The lower level controller is designed to distribute the driving force of each wheel in order to generate the required yaw moment which is calculated in the upper controller. According to 8-axle vehicle driving state, the total additional yaw moment $M_z$ is allocated based on the

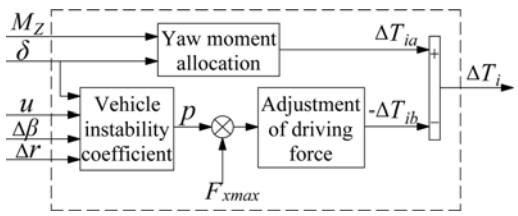


Figure 9. Schematic diagram of the lower level controller.

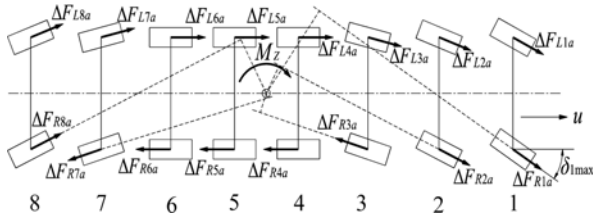


Figure 10. Lever arm of inner steering wheel around the center of mass.

rule, and the driving force for each tire is adjusted based on the principle of vehicle safety.

When the 8-axle vehicle cornering around the steering center, the length of lever arm of each steering wheel to the center of mass will change as shown in Figure 10. In order to generate the required yaw moment by the minimum adjustment of driving force of each wheel, it is necessary to consider the effect of steering angle on the lever arm and the adjusting direction of driving force.

3.3.1. Rule-based yaw moment distribution method

As shown in Figure 10, the required yaw moment $M_z$ can be calculated by the each wheel driving force. The relationship of lever arm, driving force and required yaw moment $M_Z$ is written as;

$$\sum_{i=1}^{8}\Delta F_{Lia}l_{Li}-\sum_{i=1}^{8}\Delta F_{Ria}l_{Ri}=M_z \tag{23}$$

$$\Delta F_{Lia}=\mathrm{sgn}(M_Z)(-1)^{mi}\left|\Delta F_{Lia0}\right| \tag{24}$$

$$\Delta F_{Ria}=-\mathrm{sgn}(M_Z)(-1)^{ni}\left|\Delta F_{Ria0}\right| \tag{25}$$

where, $m_i$, $n_i$ is the lever arm coefficient of left and right wheel respectively. If the lever arm of ith-axle wheel is the same as that of the first axle wheel, the $m_i$, $n_i$ will be 0; otherwise, the value of $m_i$, $n_i$ will be 1.

The adjustment of driving force $\Delta F_{Lia}$, $\Delta F_{Ria}$ can be distributed according to the vertical load of each tire, thus

$$\Delta F_{Lia0}=\frac{F_{ZLi}}{\sum_{i=1}^{16}F_{Zi}}\Delta F_{a0},\ \Delta F_{Ria0}=\frac{F_{ZRi}}{\sum_{i=1}^{16}F_{Zi}}\Delta F_{a0}$$

where, $F_{ZLi}$, $F_{ZRi}$ are the dynamic loading of the left, right wheel respectively.

The lever arm of $l_{Li}$, $l_{Ri}$ can be identified by the steering angle and vehicle structure dimensions. The relationship of inner steering angle of first axle and the steering angle of ith axle is obtained as following;

$$\delta_{outi}=a\tan\left(\frac{L_{i5}\tan\delta_l}{L_{15}+B\tan\delta_l}\right),\ \delta_{ini}=a\tan\left(\frac{L_{i5}\tan\delta_l}{L_{15}}\right)$$

where, $\delta_{outi}$ and $\delta_{ini}$ are the outer and inner steering angle of ith axle respectively ($i$ = 1, 2, 3, 7, 8).

The lever arm of ith-axle inner and outer steering wheel to the vehicle center of mass can be given;

$$l_{ini}=\frac{B}{2}\cos\delta_{ini}-l_i\sin\left|\delta_{ini}\right|,\ l_{outi}=\frac{B}{2}\cos\delta_{outi}+l_i\sin\left|\delta_{outi}\right|$$

3.3.2. Adjustment of driving force based on the vehicle safety

In order to guarantee the safety of the vehicle cornering at high speed, it is necessary to reduce the driving force of each wheel, and it will lead to the vehicle speed decreasing. The additional yaw moment generated by reducing the driving force $\Delta F_{ib}$ of wheel should be 0:

$$\sum_{i=1}^{8}\Delta F_{Lib}l_{Li}-\sum_{i=1}^{8}\Delta F_{Rib}l_{Ri}=0 \tag{26}$$

$$\sum_{i=1}^{8}\Delta F_{Lib}+\sum_{i=1}^{8}\Delta F_{Rib}=\Delta F_b \tag{27}$$

where, $\Delta F_b$ is the total adjustment of driving force, it can be calculated as following;

$$\Delta F_b=pF_{x\max}$$

where, $p$ is the instability coefficient which is defined by the extent of vehicle instability, and $F_{xmax}$ is the maximum adhesive force of the road.

$$F_{x\max}=\sum_{i=1}^{16}\sqrt{\left(\mu_sF_{Zi}\right)^2-F_{yi}^2}$$

where, $\mu_s$ is the coefficient of road adhesive, $F_{yi}$ is lateral force of the tire.

The vehicle instability can be evaluated by the vehicle speed, the error of side-slip angle and yaw rate. The higher the vehicle speed, the much easier of the vehicle instability will be.

The vehicle instability coefficient $p$ is determined by three parameters $p_1$, $p_2$, $p_3$;

$$p=p_1\cdot p_2\cdot p_3$$

where, $p_1=c_1u^3$ ($p_1=1$ at the highest vehicle speed).

The vehicle is considered to be in unstable sistuation when the errors of side-slip angle and yaw-rate exceed certain limit values. The vehicle instability coefficient of $p_2$, $p_3$ are represented as asymmetric Sigmoid function respectively;

$$p_2=\frac{1}{1+e^{-c_2(|\Delta\beta|-d_2)}},\ p_3=\frac{1}{1+e^{-c_3(|\Delta r|-d_3)}}$$

where, $|\Delta\beta|$ is error of side-slip angle, $|\Delta r|$ is error of yaw rate, $c_2$, $c_3$, $d_2$, $d_3$ are related ratios.

If the lever arm of certain inner steering wheel exceeding the center of mass, the adjustment of driving force of these wheels can be handled as outer steering wheel. The adjustment of driving force of each wheel is determined according to the tire vertical force.

$$\Delta F_{inib}=\frac{F_{Zini}}{F_{Zin}}\Delta F_{inb0},\ \Delta F_{outib}=\frac{F_{Zouti}}{F_{Zout}}\Delta F_{outb0}$$

where, $F_{Zin}$, $F_{Zout}$ are the sum of vertical force of 8-$j$ inner wheels, and 8-$j$ outer wheels respectively, $j$: the number of these inner steering wheel.

Thus, the decreasing amount of driving force, $\Delta F_{Lib}$, $\Delta F_{Rib}$, in Equations (26) and (27), is defined as follows;

$$\Delta F_{Lib} = \begin{cases} \Delta F_{inib} & \delta_l < 0 \\ \Delta F_{outib} & \delta_l > 0 \end{cases}, \quad \Delta F_{Rib} = \begin{cases} \Delta F_{outib} & \delta_l < 0 \\ \Delta F_{inib} & \delta_l > 0 \end{cases}$$

The actual driving force of each wheel $F_{Lxi}$, $F_{Rxi}$ is expressed as;

$$F_{Lxi} = F_{Lxi0} + \Delta F_{Li}, \quad F_{Rxi} = F_{Rxi0} + \Delta F_{Ri}$$

where, $F_{Lxi0}$, $F_{Rxi0}$ is the initial distribution driving force of left wheel, right wheel before the vehicle controlled by yaw moment. The adjustment of driving force of each wheel $\Delta F_{Li}$, $\Delta F_{Ri}$ is expressed as;

$$\Delta F_{Li} = \Delta F_{Lia} - \Delta F_{Lib}, \quad \Delta F_{Ri} = \Delta F_{Ria} - \Delta F_{Rib}$$

where, the $\Delta F_{Lia}$, $\Delta F_{Ria}$ is the adjustment of driving force of left side and right side wheel which is calculated with Equations (24) and (25).

### 3.4. Wheel Slip Controller

The driving force of each wheel is limited by the performance of the in-wheel driving motor, the actual output torque of driving wheel is;

$$T_{xi} = (\min < F_{xi}, F_{lim} >) \cdot r_r$$

where, $F_{xi}$: the driving force of the wheel after yaw moment distribution, $F_{lim}$: the maximum driving force of the motor supplied, $r_r$: the rolling diameter of the wheel.

The wheel slip controller is to control the wheel slip to the target value, and keep the slip ratio of each wheel below the maximum slip ratio which is determined by the road friction coefficient. For the independent in-wheel motor drive vehicle, in the case of high slip ratio above maximum slip ratio, the wheel slip controller will calculate the new output torque to adjust the slipping wheel based on the motor direct torque control method. A PID controller is adopted in this paper to regulate each wheel slip ratio following the target slip ratio.

## 4. TIRE WEAR ANALYSIS OF EACH WHEEL UNDER DRIVING CONTROL ALGORITHM

The longitudinal and lateral force of the tire will be different if the vehicle is controlled by DYC or without control. Apart from the stability state of vehicle improved, the tire characteristic will be varying and should be evaluated under these different control algorithm. The wear rate of tire is an important index which it relates with the force of the tire, the tire longitudinal slip ratio, and side slip angle of the wheel, etc.

Tire wear is proportional to the frictional work, which can be defined as;

$$W = \int_0^S F_t \cdot dl \tag{28}$$

where, $W$ represents the frictional work.

The tire force $F_t$ acting on the contact area between the tire and road consists of longitudinal force $F_x$ and lateral force $F_y$. The frictional work for a vehicle steady-state longitudinal and lateral maneuver can be described as;

$$W = \int_0^S F_x \cdot dx + \int_0^S F_y \cdot dy \tag{29}$$

The tire wear can be estimated precisely by the local contacting condition which is determined by the contact forces and slip velocities.

The relative longitudinal displacement and lateral displacement of wheel can be expressed in the terms of the longitudinal slip velocity $V_x$ and lateral slip velocity $V_y$ respectively;

$$dx = V_{sx} \cdot dt = \lambda \cdot V_x \cdot dt = \lambda \cdot ds_x, \quad dy = V_{sy} \cdot dt \tag{30}$$

where, $\lambda$ the longitudinal slip ratio, and $\alpha$ side slip angle of the wheel.

For small side slip angle of the wheel, it can be approximated as;

$$\tan(\alpha) \approx \alpha = \frac{V_{sy}}{|V_x|} \approx \frac{V_y}{|V|} \tag{31}$$

Thus, $dy = \alpha \cdot V \cdot dt = \alpha \cdot ds_x$

The tire wear is mainly related with the abrasive wear, it is a function of vertical load, tire pressure for a given tire type. The frictional work $W$ can be expressed as;

$$W = C_0 + \varepsilon \frac{S_0}{S}\left(\frac{P}{P_0}\right)^n [(\int_0^S F_x \cdot \lambda \cdot b_x \cdot \mathrm{d}s_x)^2 + (\int_0^S F_y \cdot \alpha \cdot b_y \cdot \mathrm{d}s_x)^2] \tag{32}$$

where, $n$- vertical load index (bias tire: $n$ = 1.76, belted tire $n$ = 1.88); $b_x$, $b_y$ are the coefficients related with the tire material, tire structure and tire inflation pressure, etc.

The above Equation (32) indicates that the tire wear depends on load, slippage, tire force, the roughness of the road surface, the geometry structure and material properties of the tire. The wear rate of tire will be calculated under the vehicle steady-state maneuvers.

## 5. SIMULATION RESULTS

The multi-body dynamics model of 8-axle vehicle is constructed in ADAMS/View, and the proposed driving controller is developed in the Matlab/Simulink. The co-simulation of ADAMS/View and Matlab/Simulink is built to verify the effectiveness of stability control algorithm and calculate the wear rate of tire.

The stability response of 8-axle vehicle implemented

with the controller is simulated and compared with different simulation cases. Case 1: drive torque are evenly distributed on each wheel, the vehicle has equipped with the mechanical transmission(M-drive). Case 2: the optimal torque distribution on each wheel, the vehicle has equipped with independent in-wheel motor drive wheel (E-drive).

5.1. Performance of 8-axle Vehicle under the DYC

The simulation of vehicle double lane maneuver is performed under the driver closed-loop following control. The tire-road friction coefficient is set to 0.4. The driver accelerates the vehicle speed to 80 km/h by pushing the accelerator pedal, and then keeps the angle of accelerator pedal constant. In order to analyze the vehicle performance of E-drive under DYC, we let the vehicle speed of M-drive (case 1) following the vehicle speed of E-drive (case 2) as shown in Figure 11 (a).

Figures 11 (b) and (c) present the yaw rate and side-slip angle of the center of mass. The different driving torque of each wheel (Figure 11 (d)) is used to improve the stability of the E-drive vehicle. Driving at the same speed, the drive controller of E-drive vehicle also enhances the performance over the M-drive vehicle with respect to the yaw rate error, sideslip angle and lateral position error as shown in Figures 11 (b), (c) and (e).

In Figure 11 (e), the actual trajectory of the vehicle with DYC is closer to the reference path. Figure 11 shows that the safety of vehicle can be enhanced with the proposed controller. The maneuverability performance of the vehicle under the stability control algorithm will be improved by reducing the yaw rate error and the side-slip angle.

5.2. Tire Wear Rate of 8-axle Vehicle under the DYC

The longitudinal and lateral tire force and vehicle speed can be obtained from the multi-body dynamics model of the vehicle, thus the wear rate of tire can be calculated by Equation (32).

The wear of tire is related with the load of tire as shown in Equation (32), and in reality the wheel vertical load of 8-axle vehicle is statically indeterminate problem. The independent suspension stiffness of each wheel in this paper is the same, the vertical force of tire will be determined by the vehicle spring mass and the distance of axle to the center of mass. The calculating results show the vertical load of each tire increasing from 1th axle to the 8th axle.

The steady-state lateral maneuver of vehicle is used to evaluate the wear rate of the tire. Each tire wear of the vehicle is evaluated under the different vehicle speed and road friction coefficients. Initial longitudinal vehicle speed is set to 20 km/h (inner steering angle of 1th-axle wheel: 30°), 40 km/h (inner steering angle of 1th axle wheel: 15°), 60 km/h (inner steering angle of 1th-axle wheel: 10°) respectively, and steering input is step steer. The outer tires of each axle are used for analyzing the effect of stability control algorithm on the tire wear rate.

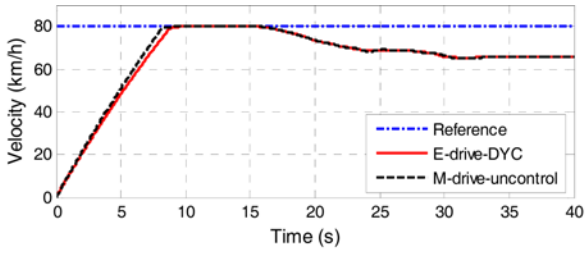


(a) Vehicle speed (km/h)

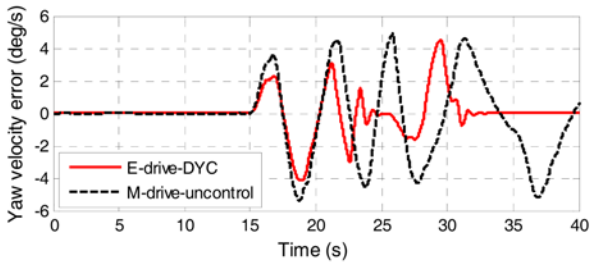


(b) Yaw rate error (deg/s)

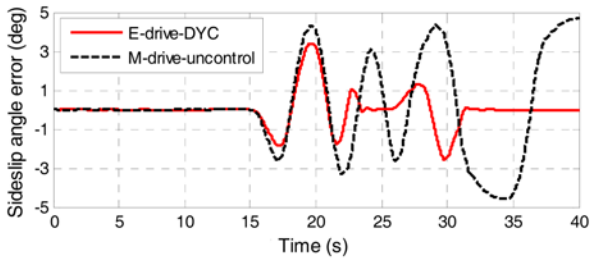


(c) Side-slip angle error (deg)

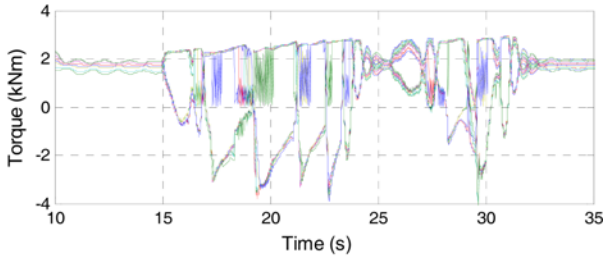


(d) Driving torque of each wheel under DYC (kNm)

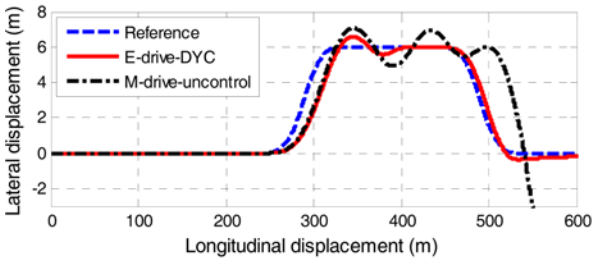


(e) Path-following trajectory

Figure 11. 8-axle vehicle under stability control.

If the vehicle step steering at the 20 km/h, 40 km/h, 60 km/h with road friction coefficient 0.8, the tire wear of each axle is shown in Figures (12) and (13). The simulation results show that the wear of tire at 6th axle is much

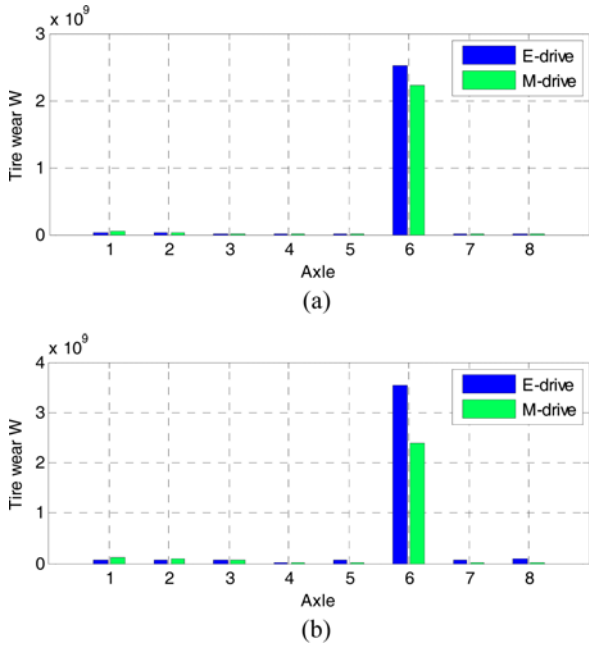


Figure 12. Wear of tire for vehicle speed = 20 km/h: (a) Adhesive friction = 0.8; (b) Adhesive friction = 0.4.

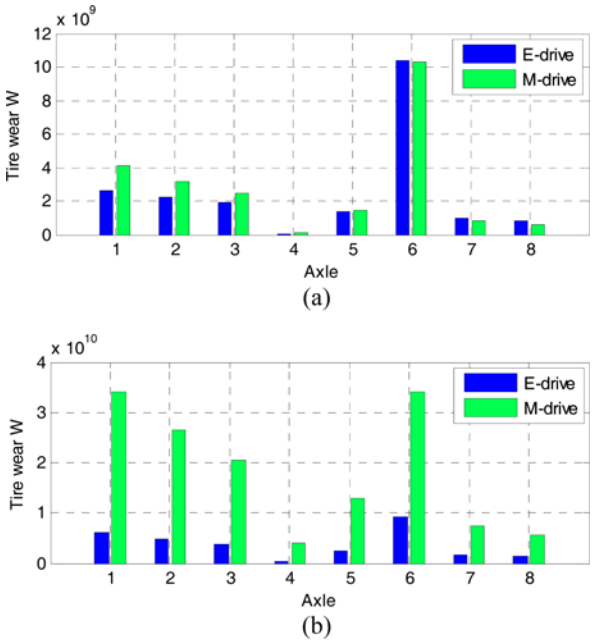


Figure 13. Wear of tire for adhesive friction = 0.8: (a) Vehicle speed = 40 km/h; (b) Vehicle speed = 60 km/h.

heavier than other tires in each situation. This may because that the 6th-axle wheel is unsteering wheel and the distance between the axle and the vehicle center of mass is larger, thus the side-slip angle and the lateral force of the wheel are much larger than that of other axle wheels during the vehicle cornering. The wear of tire for the vehicle with the optimal torque distribution (E-drive) is almost the same to that of mechanical differential (M-drive) for the lower vehicle speed (20 km/h). As the vehicle speed becoming higher, this trend will be opposite. When the vehicle speed up to 60 km/h, the wear of tire for the vehicle with the optimal torque distribution (E-drive) is much less than that of the vehicle with mechanical differential (M-drive). This mainly because that the optimal torque distribution of the wheel will lead the vehicle speed decreasing to maintain the stability of the vehicle as shown in Figure 11.

When the vehicle cornering at the 20 km/h with road friction coefficients 0.4, the tire wear rate of each axle of the vehicle with electrical differential (E-drive) is little heavier than that of vehicle with the mechanical differential (M-drive). This may be the tire force (longitudinal and lateral force) in this situation is lower than that of road friction coefficients 0.8.

The stability control of vehicle will not only improve the dynamic behavior of the vehicle, but also affect the wear rate of tire. In order to decrease the maintenance costs of the vehicle, the control objective may be include the stability of vehicle and the wear rate of tire.

## 6. CONCLUSION

The stability and maneuverability of the 8-axle vehicle improved by the driving control algorithm is presented in this paper. The 3-D multi-body dynamics model of the vehicle is built in ADAMS which can have the transient behavior of road-tire interaction force. The optimal torque distributed to each wheel of 8-axle vehicle is determined by hierarchical controller which considering the friction force acting on the tire-road, dynamic load of tire and motor output capability. In the upper level controller, the feed-forward and feed-backward control theory is used to compute control yaw moment. The fuzzification of feed-forward controller is designed with considering the yaw rate and side-slip angle of the center of mass simultaneously. In the lower level controller, the control yaw moment is distributed to each wheel based on rule-law and the vehicle safety driving principle. It has been shown that the stability response of 8-axle vehicle can be improved by the proposed hierarchical controller.

The wear rate of each tire of the 8-axle vehicle is analyzed by quantitatively under the stability control algorithm. The simulation results demonstrate that wear rate of tire belonging to 6th axle is much heavier than the other axles'. The wear of tire is different for the vehicle controlled by DYC or not. If the vehicle steering at the low speed, the vehicle with equal distribution of driving force will show the advantage in the aspect of tire wear. The wear of tire will be lighter when the vehicle controlled by DYC cornering at the high speed. It is worth noting that the wear of tire can be an index for evaluation the performance of vehicle stability control algorthim.

**ACKNOWLEDGEMENT**–This research was supported by the

National High Technology Research and Development Program of China (863 Program) (Grant No. 2011AA060404).

## REFERENCES

Alipour, H., Sabahi, M. and Sharifian, M. B. B. (2014). Lateral stabilization of a four wheel independent drive electric vehicle on slippery roads. *Mechatronics*, **30**, 275–285.

An, S. J., Yi, K., Jung, G., Lee, K. I. and Kim, Y. W. (2008). Desired yaw rate and steering control method during cornering for a six-wheeled vehicle. *Int. J. Automotive Technology* **9**, **2**, 173−181.

Boada, B. L., Boada, M. J. L. and Diaz, V. (2005). Fuzzy-logic applied to yaw moment control for vehicle stability. *Vehicle System Dynamics* **43**, **10**, 753−770.

Da Silva, M. M., Cunha, R. H. and Neto, A. C. (2012). A simplified model for evaluating tire wear during conceptual design. *Int. J. Automotive Technology* **13**, **6**, 915−922.

Kim, W. G., Kang, J. Y. and Yi, K. (2011). Drive control system design for stability and maneuverability of a 6WD/6WS vehicle. *Int. J. Automotive Technology* **12**, **1**, 67−74.

Kim, W., Yi, K. and Lee, J. (2011). Drive control algorithm for an independent 8 in-wheel motor drive vehicle. *J. Mechanical Science and Technology* **25**, **6**, 1573−1581.

Kim, C. J., Mian, A. A., Kim, S. H., Back, S. H., Jang, H. B., Jang, J. H. and Han, C. S. (2015). Performance evaluation of integrated control of direct yaw moment and slip ratio control for electric vehicle with rear in-wheel motors on split-mu road. *Int. J. Automotive Technology* **16**, **6**, 939–946.

Li, L., Jia, G., Chen, J., Zhu, H., Cao, D. and Song, J. (2015). A novel vehicle dynamics stability control algorithm based on the hierarchical strategy with constrain of nonlinear tyre forces. *Vehicle System Dynamics* **53**, **8**, 1093–1116.

Özkan, B., Aptoula, E., Heren, T., Mandacı, H. and Can, Ç. (2014). Minimization of tire wear for tractor semi-trailers with command steering. *Otomotiv Teknolojileri Kongresi*. Bursa, Turkey.

Sill, J. H. and Ayalew, B. (2011). Managing axle saturation for vehicle stability control with independent wheel drives. *American Control Conf. (ACC)*, 3960–3965.

Williams, D. E. (2012). Generalised multi-axle vehicle handling. *Vehicle System Dynamics* **50**, **1**, 149–166.

Williams, D. E. (2014). Lane-keeping benefits of practical rear axle steer. *Vehicle System Dynamics* **52**, **4**, 504–521.

Yin, G., Wang, R. and Wang, J. (2015). Robust control for four wheel independently-actuated electric ground vehicles by external yaw-moment generation. *Int. J. Automotive Technology* **16**, **5**, 839–847.

Zong, C. F., Li, W. and Zheng, H. Y. (2014). A control algorithm of braking force distribution for EBS based on dynamic axle load. *Automobile Technology* **2014**, **1**, 20-23+48.

Zuo, S. G., Ni, T. X., Wu, X. D., Wu, K. and Yang, X. W. (2014). Prediction procedure for wear distribution of transient rolling tire. *Int. J. Automotive Technology* **15**, **3**, 505−515.